RSC Advances

PAPER

View Article Online
View Journal | View Issue

Cite this: *RSC Adv.*, 2022, **12**, 25465

Catalytic conversion of heavy naphtha to reformate over the phosphorus-ZSM-5 catalyst at a lower reforming temperature†

Emad N. Al-Shafei,* Mohammed Z. Albahar,* Mohammad F. Aljishi, Aaron Akah, Ali N. Aljishi and Ahmed Alasseel

Naphtha reforming to aromatics, naphthenes, and iso-paraffins is an essential process to increase the octane number of gasoline through the utilization of middle naphtha (whole). A ZSM-5 zeolite catalyst with modified medium pores was developed to comprehend the existing limitation of catalytic reforming to the unutilized refinery feedstock of heavy naphtha. The study applied a lower reforming conversion temperature (350 °C) than a conventional reformer without noble metal addition in an effort to lower the carbon footprint of the process and catalyst cost. The modified zeolite catalyst was impregnated with phosphorus oxide and spray-dried, followed by a hydrothermal treatment with steam. The parent and modified catalysts were characterized by NH_3-TPD, SEM, XRD, NMR, FTIR, and N_2 physisorption. Steam treatment was conducted to reduce the original zeolite acidity, mainly in the form of Brønsted acid sites, which resulted in the formation of phosphorus–aluminum species in the framework. The modified catalyst consisting of 40% ZSM-5 and 60% binder delivered high conversion of dodecane, and the reforming reaction selectivity favored the formation of carbonium ions through β-scission. Therefore, monomolecular cracking took place, resulting in the production of olefins and paraffin alongside iso-paraffins, aromatics, and naphthenes, which are associated with the bimolecular pathway. The reforming of heavy naphtha was different; the free radicals from β-scission were affected by the surrounding molecules of feedstock, and the bimolecular reactions were more dominant through zeolite pores. The study demonstrated that the addition of 10% steam during the reaction of heavy naphtha suppressed coke formation. Furthermore, high conversion and steady selectivity were maintained during the reaction, which resulted in gasoline reformate with a high research octane number (RON).

Received 2nd July 2022
Accepted 19th August 2022

DOI: 10.1039/d2ra04092a

rsc.li/rsc-advances

1. Introduction

Gasoline blends of most refineries often depend on naphtha catalytic reforming units as they produce reformate gasoline with high octane numbers.[1,2] To enhance the octane number and improve product quality, straight run light naphtha (boiling point 35–93 °C) and middle (whole) naphtha (boiling point 93–157 °C) are normally sent to either isomerization catalytic reactors or naphtha catalytic reforming units prior to gasoline blending. However, these processes cannot tolerate sulfur compounds, and thus, the feedstock naphtha must be hydrotreated to remove organic sulfur before feeding it to the catalytic reactor. During the naphtha reforming by the conventional reforming process, high reaction temperatures ranging between 450 and 480 °C are applied to reform middle naphtha feedstock fraction having low octane numbers between 35 and 50. The process is essential for all refineries as it leads to obtaining gasoline products with high octane numbers ranging from 70 to higher than 100 under hydrogen pressure (5–45 atm).[3,4] In reforming units, depending on reaction conditions, catalysts such as Pt–Re–$A1_2O_3$, Pt–Sn–$A1_2O_3$,[4] and Pt–Cl–$A1_2O_3$ (ref. 5) are used to enhance the overall aromatic yield to around 70 wt%, with a focus on improving the yields of benzene, toluene, and xylene (BTX) in the product.[6]

Several zeolite catalysts, with well-defined microporous channel structures consisting of Si–Al oxides, are applied in different major hydrocarbon conversion processes in the petrochemical and refining industry.[7] Their unique properties, such as hydrothermal stability and strong acidity, allow them to be used in many shape selective reactions.[8,9] However, the main challenge with the application of zeolites in refining and petrochemical processes is the formation of coke due to the blockage of pores by bulky molecules, which increases the deactivation rate of the catalyst.[10–12] The reactivity of zeolites is known to be linked to its acidity, which arises from the bridging hydroxyl groups associated with the aluminum in the framework. The protons at these sites provide Brønsted acid sites and

Research and Development Center, Saudi Aramco, Dhahran 31311, Saudi Arabia. E-mail: emad.shafei@aramco.com; emadnaji@gmail.com

† Electronic supplementary information (ESI) available. See https://doi.org/10.1039/d2ra04092a

are mostly located inside the pores. Lewis acid sites also play a role in catalytic reactions through activation and polarization of the adsorbed molecules.[13–15]

Several studies investigated the application of zeolites for naphtha reforming, both as support and as a catalyst. Zhang *et al.*[16] utilized impregnated Y-zeolite-based catalysts with Pt–Ce, Pt–Mg, Pt–Ba, and Pt–Ti for naphtha reforming at 490–510 °C and H_2 pressure of 0.7 MPa. It was observed that the production of aromatics increased significantly due to the strong acidity of zeolite, exceeding results typically achieved by commercial catalysts.[16,17] Moreover, Karakoulia *et al.* utilized Pt–Ni/beta[18] and Pt-/AlSBA-15-BET[19] zeolite for the hydroisomerization of *n*-octane and a naphtha stream under hydrogen pressure with a lower reaction temperature (260–300 °C) than the conventional catalytic reforming reaction.[20] The moderate acidity of the utilized Pt–Ni/beta-zeolite catalyst improved the octane number of naphtha from 55 to 62. Furthermore, the bimetallic catalyst was found to assist the hydroisomerization reaction.[18,19] Shammari *et al.*[21] investigated the effects of medium pore ring ZSM-5 and large pore ring mordenite zeolites as acidic catalysts in naphtha reforming to gasoline by studying several model compounds (ethylbenzene, iso-octane, and dodecane). Reactions were conducted in a fluidized-bed reactor at atmospheric pressure and a reaction temperature of around 400 °C. Their kinetic studies showed that the hydrocarbon cracking rate is affected not only by the zeolite structure but also by the paraffinic or non-paraffinic nature of the model compounds. Additionally, higher activation energy was obtained over ZSM-5 for the conversion of dodecane and ethylbenzene.[22–25]

Several zeolite modifications have been studied to overcome the zeolite deactivation by coke, such as hydrothermal treatment, desilication, or dealumination methods.[22,26–29] Steam treatment is normally performed on the zeolite to create more mesopores in the structure and has been broadly used for FCC zeolite catalysts to improve their catalytic cracking stability.[26] Higher temperature steaming of zeolites may cause framework dealumination and consequently affect the textural properties.[26] However, steaming has been reported to modify the catalytic acidic sites of zeolites and improve the reaction stability. Furthermore, it has been demonstrated that mild steaming can produce efficient acidic sites. Dealuminating the catalyst by steaming can lead to the formation of a secondary pore structure, which can improve the aromatization stability by reducing diffusion limitations.[30] For example, Almutairi *et al.* found that the change in the outer region of the zeolite structure, as a result of steaming, improved the accessibility to Brønsted acid sites. Moreover, the steaming caused a decrease in the quantity of Brønsted acid sites, which slowed coke formation. Therefore, a higher turn-over frequency of reactant molecule per Brønsted acid site was achieved.[30,31] Wang *et al.*[32] studied the influence of steaming on the catalytic activity and physio-chemical properties of ZSM-5. It was concluded that dealumination reduced the amount and strength of acid sites as well as the Brønsted to Lewis acid sites ratio.[33] In addition, it was found that an optimal aromatic yield can be achieved with moderate Brønsted/Lewis acid sites, which can be reached *via* steam treatment. The newly formed mesopores and the low acidity of steam-treated ZSM-5 enhanced the stability of the catalyst (over 50 h) and increased the yield of aromatics.

Impregnating ZSM-5 with phosphorus represents an alternative modification method designed to improve the hydrothermal stability of the catalyst and modify its acidity and selectivity towards selected products.[34] Phosphorus interacts with the acid sites of zeolites leading to a decrease in their number and strength and thus reducing the rate of coke formation. Phosphorus in zeolites can be found in different phases, which include (i) separate phosphate and zeolite phases (ii) phosphate interacting with framework aluminum in the zeolite (iii) a phosphate interacting with extra framework aluminum.[34] It was shown by different characterization techniques that phosphorus species are concentrated more on the zeolite surface than on the catalyst's pores. To overcome such non-uniform distribution, phosphorus can be incorporated into the zeolite catalyst through the hydrothermal dispersion technique (*i.e.*, stirring phosphorus solution with a catalyst at a temperature around 60 °C), which results in a more homogenous dispersion of phosphorus throughout the pores and channels of the zeolite. Furthermore, applying steam treatment to the phosphorus-modified zeolite results in an increased phosphorus concentration on the surface area. This suggests that some of the pore acidity is recovered during steaming as some internal phosphorus species migrate to the external surface.[35]

Industrially, zeolites are often dispersed in a binder and shaped based on the needs of specific reactions. Binders are essential for catalyst scale-up and may provide more porosity and surface acidity to assist in various reactions under catalytic and thermal cracking conditions.[36] Song *et al.* studied the modification of extruded ZSM-5 with phosphorus oxide and its effect on changing the acidity and activity of the catalyst, both before and after steaming.[36] The interaction between the zeolite, binder, and phosphorus species before and after the steam treatment was studied, and they observed that the formation of phosphorus hydroxyl bonds with Al-hydroxyls decreased the number of Lewis acid sites associated with the binder. Furthermore, the Brønsted acid sites of ZSM-5 were reduced as some of the phosphorus species interacted with the tetrahedral framework aluminum. It was concluded that the steam phosphorus-modified ZSM-5 delivered the highest selectivity and longest lifetime.[36]

Reforming of dodecane was performed over various catalysts, including modified MFI and beta zeolites, to investigate the effect of medium and large pore structure and different 3D sinusoidal microporous channels as well as different modifications on pore selectivity and activity.[27,28,37] Ishihara *et al.*[38] focused on improving the gasoline octane number through dodecane cracking over Y and beta zeolites. It was observed that high yields of gasoline were achieved at high conversions, and beta zeolite delivered higher conversion than Y-zeolite. Furthermore, several studies investigated the ZSM-5 zeolite for aromatization reactions and concluded that the catalytic activity and selectivity were enhanced due to the distinctive channel structure dimensions of ZSM-5 and its acidic properties.[39–41]

In general, it is well recognized in the literature that the reaction pathway over zeolites follows either monomolecular

cracking or bimolecular reaction.[42,43] The cracking mechanism involves the formation of carbonium ions as intermediates. Initially, a carbonium ion is formed through the addition of a proton on a saturated molecule or a double bond resulting in the formation of a penta-coordinated ion, which cracks into the paraffin and a carbonium ion. Then, the carbonium ion is cracked into an olefin and a smaller carbonium ion through monomolecular cracking.[42] Alternatively, the reaction can proceed *via* a bimolecular mechanism, in which a feed molecule reacts with a carbonium ion to form a larger molecule. Large pore rings of zeolites Y and beta are well-known catalysts for cracking bulky hydrocarbon molecules and are deployed in different fluid catalytic cracking (FCC) processes. These large pore zeolites can facilitate bimolecular reactions.[44–46] On the other hand, monomolecular cracking is predominant over the medium pore ring of ZSM-5 due to its medium pore size. Moreover, the formation of smaller olefins such as ethylene and propylene is favored over ZSM-5.[42,43,47,48]

Multiple operational variables influence the performance of the catalytic naphtha reforming process, including temperature, pressure, feed rate, and hydrogen partial pressure.[3] Decreasing the energy requirements and operating at low pressures is one of the major factors in improving the performance of continuous catalytic reforming (CCR).[49] Fired heaters require substantial amounts of fuel to run the naphtha reforming process. In addition to high energy consumption in the pre-heaters, utilizing higher temperatures introduces high costs, as it requires high temperature-resistance materials for manufacturing reactors and equipment.[50] On the other hand, operating at high hydrogen partial pressures has been found to result in the reduction of aromatic production and a decline in the RON of the final product.[3]

Therefore, to overcome such limitations, the motivation of this study is to investigate new catalysts for heavy naphtha utilization and reforming that enable operating at lower reactor temperatures,[51] without the utilization of noble metals, no hydrogen pressure,[51] and lower than conventional reforming (450 and 480 °C), in an effort to reduce the carbon footprint of the process. Specifically, this study aims to improve the catalytic performance of MFI zeolite for the catalytic reforming of heavy naphtha to gasoline at atmospheric pressure and a low reaction temperature of 350 °C. The zeolite was impregnated with phosphorus oxide and subjected to steam treatment to enhance its performance in terms of conversion stability and deactivation behavior during the reaction through the modification of its acidity. The modified zeolite was analyzed by different characterization techniques to study the changes in physical and chemical properties. Moreover, results from this study will further enhance our understanding of reaction pathways, including both primary cracking and secondary reactions, such as transalkylation and cyclization.

2. Experimental

2.1 Catalyst preparation

MFI commercial zeolite in the ammonium form, ZSM-5 (silica alumina ratio, Si/Al = 23), was obtained from Zeolyst and calcined in air at 575 °C for 5 h. The zeolite catalyst was impregnated with phosphorus oxide using *ortho*-phosphoric acid (H_3PO_4: 85 wt% in H_2O, Sigma Aldrich). The modification was performed by gradually adding the required diluted H_3PO_4 (0.5 N) to load 1.5 wt% P_2O_5 on the catalyst. The stirring was continued for 15 min prior to mixing with the binder to form spheres. The preparation of zeolite catalysts was as follows: firstly, a slurry was formed by mixing 30 wt% kaolin clay powder (Sigma Aldrich) with deionized water. In a separate step, another slurry mixture was made, consisting of a parent or modified zeolite (40 wt%) and deionized water, which was stirred continuously for 15 min. Then, the zeolite slurry was added to the kaolin slurry and stirred for an additional 5 min. After that, a separate slurry was prepared by mixing 30 wt% Catapal alumina (Sasol) with distilled water and 0.5 wt% diluted nitric acid (0.2 N) and was kept stirring for 30 min. The resulting slurry was added to the zeolite-kaolin slurry and mixed for 15 min to produce a highly viscous slurry, which was then spray-dried using GEA Niro spray-drier. Finally, the formed spheres were calcined at 500 °C for 6 h. To investigate the effect of steaming, all formulated zeolite spheres in this study were subjected to hydrothermal treatment with steam. This was performed by introducing steam (100 °C) bubbled through nitrogen flow (100 ml min^{-1}) as a carrier gas over the catalyst at 700 °C for 8 h in a tube furnace, after which the flow of steam was stopped, and the catalyst was purged with nitrogen for 3 h. After cooling to room temperature, the samples were labelled as parent zeolite (P), modified zeolite with phosphorus oxide (P-ZSM-5), modified zeolite with phosphorus oxide binder (P-ZSM-5-B), and zeolite hydrothermally treated with steam was denoted as (HT).

2.2 Catalyst characterization

The textural properties of zeolite and zeolite binder mixture were analyzed by N_2 adsorption using ASAP 2420 Micromeritics surface analyzer to obtain the surface area, pore volume, and pore size distribution. Samples were pre-heated in a vacuum at 300 °C for 4 h prior to analysis, and the generated *t*-plot was calculated according to Harkins and Jura equation. The X-ray diffraction patterns of all zeolites were obtained using Panalytical X'Pert PRO diffractometer consisting of copper-anode tube radiation with a wavelength of 1.5418 Å. The environmental scanning electron microscope (ESEM) was utilized to study the surface topology of the zeolite spray-dried particles by FEI Quanta 400 instrument equipped with EDAX super-ultra-thin detector for metal analysis and operating at 20 kV with no coating required.

Measuring the acidity of the catalysts is crucial to comprehend their catalytic behavior. Therefore, temperature-programmed desorption of ammonia (NH_3-TPD) experiments were carried out to evaluate the total acidity of the zeolite catalysts. Prior to the analysis, zeolite samples were pre-heated to 550 °C under helium and then cooled prior to the adsorption of NH_3. The desorption of ammonia at different temperatures from 100 to 550 °C was measured by a thermal conductivity detector (TCD) using Micromeritics Autochem 2910. The

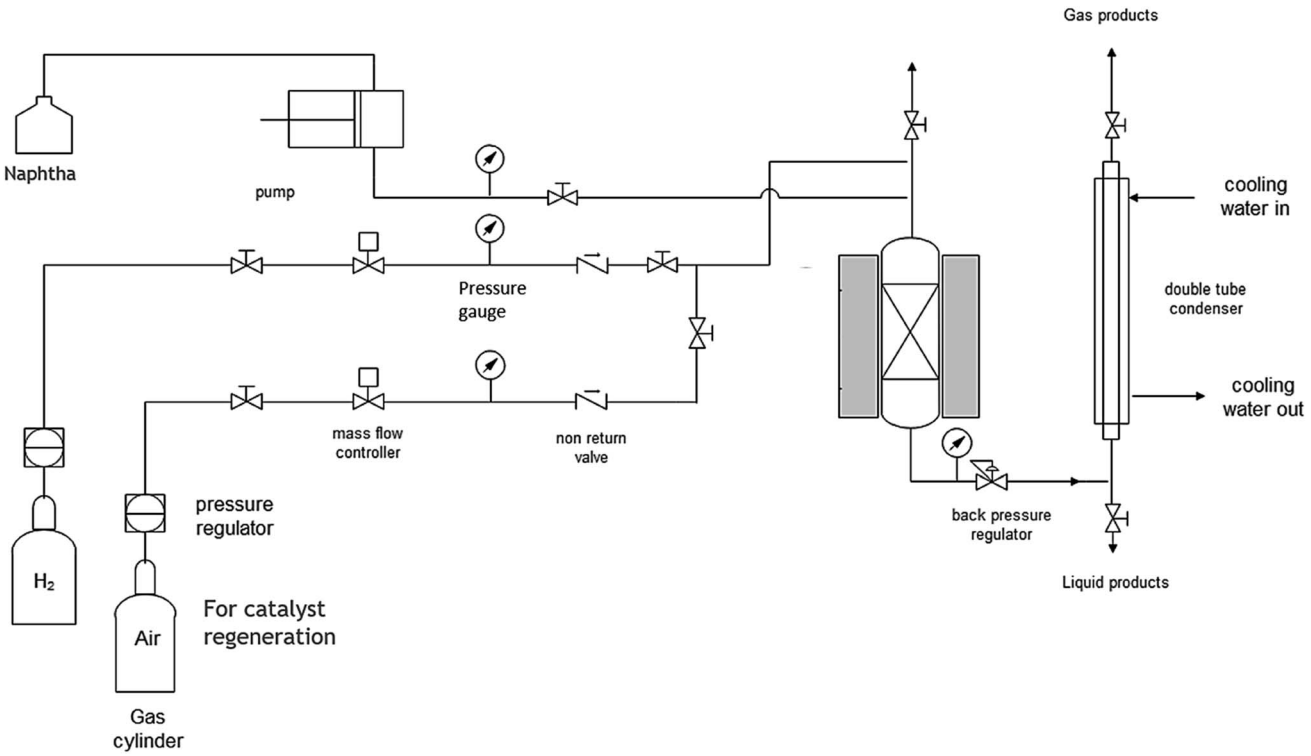

Fig. 1 Reaction system schematic and configuration.

amount of acid sites was calculated by using predetermined standard response factors to measure the peak area before and after the hydrothermal treatment of zeolite binder mixture catalysts with steam. Furthermore, due to their different acidic behavior during the catalytic reactions, it is important to define the type of acid sites formed in the catalyst, both Brønsted acid sites (BAS) and Lewis acid sites (LAS). Therefore, Fourier transform infrared (FTIR) spectroscopy was employed for 40% ZSM-5 in 60% binder after steam treatment. Zeolite catalyst samples (30 mg) were pressed in a self-supported wafer and heated to 500 °C for 30 min under vacuum and then cooled to 150 °C. Then, 40% of the zeolite catalyst wafer was exposed to pyridine (py) vapor at 150 °C to determine BAS and LAS. The observed peaks at ~1540 and 1450 cm^{-1} are represented by py-BAS and py-LAS, respectively.

Magic angle spinning nuclear magnetic resonance (MAS NMR) was utilized to obtain information on the number and type of neighboring atoms and bonding characteristics from the created chemical shift (δ) data. It was difficult to study the effect of steam treatment and phosphorous addition on the mixed zeolite framework with binder due to the high concentrations of alumina from the binder matrix. Therefore, ZSM-5 without a binder was impregnated with 1.5 wt% P_2O_5 and hydrothermally treated with steam to study the effect of modification on the zeolite framework. Selected zeolite samples were analyzed by solid state ^{27}Al and ^{31}P MAS NMR. Varian 500 MHz nuclear magnetic resonance spectrometer equipped with a 4 mm solid HX probe was utilized. Finally, the amount of deposited coke over the zeolite samples after catalytic activity testing was measured by a PerkinElmer 2400CHN elemental analyzer.

2.3 Catalytic activity evaluation

The catalytic cracking of dodecane and straight run heavy naphtha (boiling point of 157–202 °C) was conducted at atmospheric pressure in a packed bed reactor. Firstly, N_2 was fed as a carrier gas at a constant flow rate of 30 ml min^{-1}, and the reactor temperature was raised to 350 °C. Then, the liquid feed was injected into the reactor through a HPLC pump, and the flow rate was adjusted accordingly to achieve a liquid hourly space velocity (LHSV) of 4 h^{-1}. The study was extended to investigate the addition of 10% water by using a second HPLC pump to study the effect of steam on heavy naphtha reforming, and the centrifuge was used to separate water from the reformate product after the cold trap. The product from the reactor was trapped by a cooling water bath located downstream of the reactor. The reaction system schematic can be seen in Fig. 1. The detailed hydrocarbon analysis to determine the research octane number (RON)[52–54] and PIONA (paraffin, i-paraffin, olefin, naphthene, aromatic) was performed by applying the ASTM method D5134 using a gas chromatograph (GC) from Agilent. It is equipped with a flame ionization detector (FID) to determine the reaction conversion and selectivity.

3. Results and discussion

3.1 Phase identification and morphology

The acquired SEM images of the catalyst consisting of 40% ZSM-5 in 60% binder show well-formed spherical particles having an average size of 8.9 μm, as illustrated in Fig. 2A. The XRD analysis showed the diffraction patterns of ZSM-5 zeolite mixed with a binder after being hydrothermally treated with

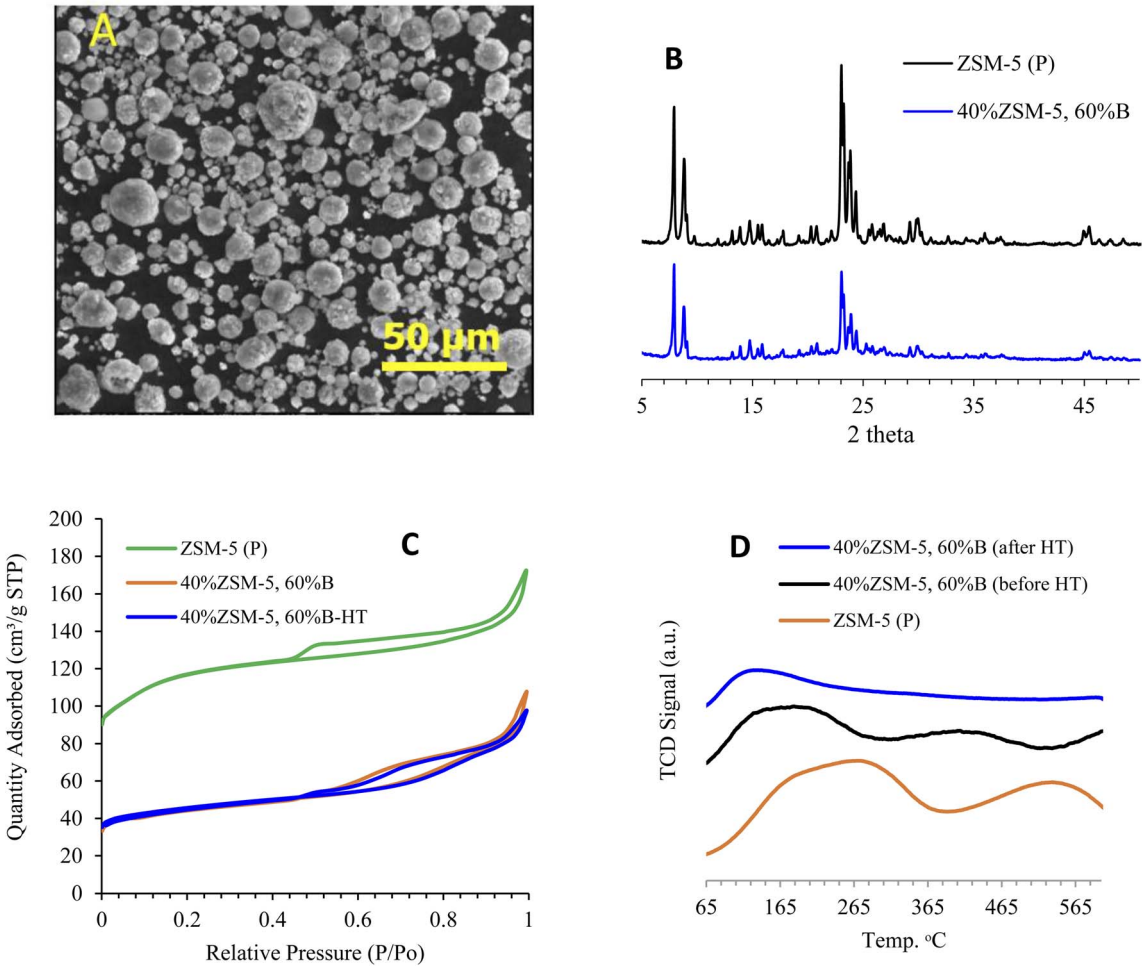

Fig. 2 [A] SEM images 40% ZSM-5 in 60% binder, [B] XRD patterns of zeolite catalysts with binder hydrothermally treated with steam, [C] N_2 adsorption–desorption isotherms of parent and modified ZSM-5 zeolite with binder, [D] NH_3-TPD of zeolites with binder and zeolites with binder hydrothermally treated with steam.

steam. Fig. 2B illustrates the main diffraction peaks of ZSM-5 zeolite (7.7–7.9° and 22.5–25°),[55] and the absence of P_2O_5 diffraction peak due to little quantity used, which suggest that the zeolite crystalline structure was neither affected by steam treatment nor by the addition of 60% binder to the framework. Fig. 2B also shows that the X-ray patterns of the parent ZSM-5 without binder and that mixed with 60% binder are both highly crystalline and identical. However, the intensity of the peaks was reduced after the addition of the binder. Fig. 2S† shows the XRD analysis of 40% ZSM-5 before and after the reaction, and it is observed that both samples are highly crystalline and identical, while the intensity of the peaks after the reaction was slightly reduced as a result of coke deposition.

3.2 Textural properties of modified ZSM-5 with binder

The nitrogen adsorption analysis measurements, tabulated in Table 1, reveal that the surface area and pore volume decreased after mixing ZSM-5 with 60% binder, with the surface area dropping from 419 to 164 $m^2\ g^{-1}$. On the other hand, hydrothermal treatment with steam resulted in a slight increase in the surface area of 40% ZSM-5 in 60% binder, from 164 to 170 $m^2\ g^{-1}$. Fig. 2C shows a drop in the adsorption/desorption isotherm curve of 40% ZSM-5 in 60% binder compared to the parent sample (ZSM-5 (P)) due to the addition of the binder matrix. Table 1S† shows that the surface area was reduced after the reaction as a result of coke deposition. It is noticeable that the microporous surface area was more affected than the external surface area. This indicates that the reaction was mainly occurring inside the pores. The microporous surface area decreased from 106 to 76 $m^2\ g^{-1}$ compared to the negligible change in the external surface area from 64 to 61 $m^2\ g^{-1}$. Furthermore, the isotherm of the post reaction sample was decreased slightly due to coke formation while the pore size distribution was virtually unchanged (Fig. 2S†).

3.3 Acidic properties of the catalysts

The zeolite acidity was measured using NH_3-TPD analysis, and Fig. 2D shows the ammonia adsorption intensities of zeolite in the binder before and after hydrothermal treatment with steam compared with ZSM-5 (P). Table 1 demonstrates the difference in total acidity of zeolite with the binder before and after hydrothermal treatment with steam. The steam treatment

Table 1 Nitrogen adsorption analysis and NH_3-TPD profiles of parent and modified ZSM-5

Zeolite ID	BET surface area [$m^2\ g^{-1}$]	*t*-Plot[a] micropore surface area, [$m^2\ g^{-1}$]	*t*-Plot[a] external surface area, [$m^2\ g^{-1}$]	Pore volume, [$cm^3\ g^{-1}$]	Total adsorption NH_3 [$\mu mol\ g^{-1}$]	LT[c] adsorption NH_3 [$\mu mol\ g^{-1}$]	HT[d] adsorption NH_3 [$\mu mol\ g^{-1}$]
ZSM-5 (P)	419	254	165	0.27	2048	1250	798
40% ZSM-5, 60% binder	164	103	61	0.16	980.8	668.8	312.0
40% ZSM-5, 60% binder HT[b]	170	106	64	0.15	810.4	632.0	178.4

[a] Surface area by *t*-plot derived from Harkins and Jura equation. [b] HT: hydrothermal treatment with steam. [c] Low temperature. [d] High temperature.

slightly affected the zeolite acidity concentration of low temperature adsorption, while at high temperature, adsorption strength was reduced by about ~50% of its original value before hydrothermal treatment with steam. Although the steam treatment directly impacted the zeolite acidic sites, the catalyst framework was not affected, as seen in the XRD patterns in Fig. 2B. The acidity of 40% ZSM-5 in 60% binder before and after hydrothermal treatment with steam was evaluated using FTIR with pyridine as a probe molecule. Pyridine FTIR provides qualitative information on Brønsted and Lewis acid site peaks, which are found at 1446 cm^{-1} and 1548 cm^{-1}, respectively.[56] It can be observed that hydrothermal treatment with steam reduced the acidity of the 40% ZSM-5 in 60% binder catalyst, as presented in Table 2. The increase in the number of Lewis acid sites in the steam-treated sample with the reduction in Brønsted acid sites suggests that hydrothermal treatment contributed to suppressing coke formation[57] through the transformation of some Brønsted acid sites into Lewis acid sites. Such modification of acidity is found to be significant in assisting better catalytic cracking performance. The reduction in acidity positively impacted the catalytic stability, which was maintained for a longer time on stream. Although a minimum amount of Brønsted acid sites is required to initiate the primary reaction, controlling the concentration of Brønsted acid sites is essential in preserving the zeolite shape selectivity and reactivity.[58] High amounts of Brønsted acid sites can lead to more severe catalytic cracking, which results in more coke deposition and thus a faster rate of deactivation. Fig. 4S† shows the strength of both Lewis and Brønsted acid sites, which can be determined by evaluating the acidity at different temperatures (150–450 °C) for the 40% ZSM-5 in 60% binder and the steam treated catalyst. The reduction of Lewis acid sites was found to be in the range of ~40% of both zeolite catalysts from original acidity, while the Brønsted acid sites maintained about 70% and 30%, respectively, as the temperature increased from 150 °C to 450 °C.

3.4 Framework of modified ZSM-5

The aluminum coordination was difficult to investigate by ^{27}Al MAS-NMR due to the high concentration of alumina coming from the binder. Therefore, separate experiments were conducted to investigate the effect of phosphorus and hydrothermal treatment with steam on the aluminum in the zeolite framework before mixing with the binder. Three samples without binder were compared, including hydrothermally treated (with steam) ZSM-5 impregnated with 1.5% P_2O_5, hydrothermally treated ZSM-5 without P_2O_5, and the parent ZSM-5. The ^{27}Al MAS-NMR indicated a reduction in the peak of the tetrahedrally coordinated aluminum after hydrothermal treatment with steam, as seen in Fig. 3A. The decline in tetrahedral aluminum at ~60 ppm is attributed to the reduction in Brønsted acid sites of zeolite, while the appearance of the octahedrally coordinated aluminum at ~0 ppm demonstrates the formation of Lewis acid sites after steaming of the parent ZSM-5. Furthermore, the ZSM-5 impregnated with 1.5% P_2O_5 and hydrothermally treated with steam showed a similar decline in the tetrahedrally coordinated aluminum peak.

Table 2 Lewis and Brønsted acid density derived from the adsorption by pyridine-FTIR of the zeolite catalyst

Sample name	Temperature (°C)	C_L[a] (mmol g^{-1})	C_B[b] (mmol g^{-1})	Total acidity	B/L[c] ratio
40% ZSM-5 in binder	150	0.020	0.3337	0.354	0.061
40% ZSM-5 in binder (HT)	150	0.066	0.0625	0.129	1.059

[a] Lewis acid sites. [b] Brønsted acid sites. [c] Brønsted/Lewis ratio.

However, a new peak was observed at ~40 ppm due to the formation of phosphorus–aluminum, similar to observations reported earlier by Song *et al.*[36] Furthermore, the octahedrally coordinated phosphorus–aluminum species were detected at −10 ppm.[34] Thus, the MAS-NMR analysis confirmed that the phosphorus was successfully impregnated in the zeolite framework.

Moreover, ^{31}P MAS NMR of impregnated 40% ZSM-5 in 60% binder before and after hydrothermal treatment (steam) with 1.5% P_2O_5 were compared with ZSM-5 catalyst impregnated with 1.5% P_2O_5 and hydrothermally treated with steam without binder, which was used as a reference for NMR analysis, as illustrated in Fig. 3B. Aluminophosphate species were detected in the range of −5 to −30 ppm, confirming the interaction of phosphorus with the zeolite framework in non-extruded samples. Hodala *et al.*[59] reported similar findings on a phosphorus impregnated zeolite, where the NMR spectra showed the formation of pyrophosphate, polyphosphate, and aluminophosphated species (−5.72, −22.05, and −32.87, respectively).[59] The interaction between the zeolite matrix and orthophosphate species, although no effect on the morphology, was observed after the modification of the catalyst. Specifically, they observed the formation of a more stable interaction between the zeolite and pyrophosphate, polyphosphate, and

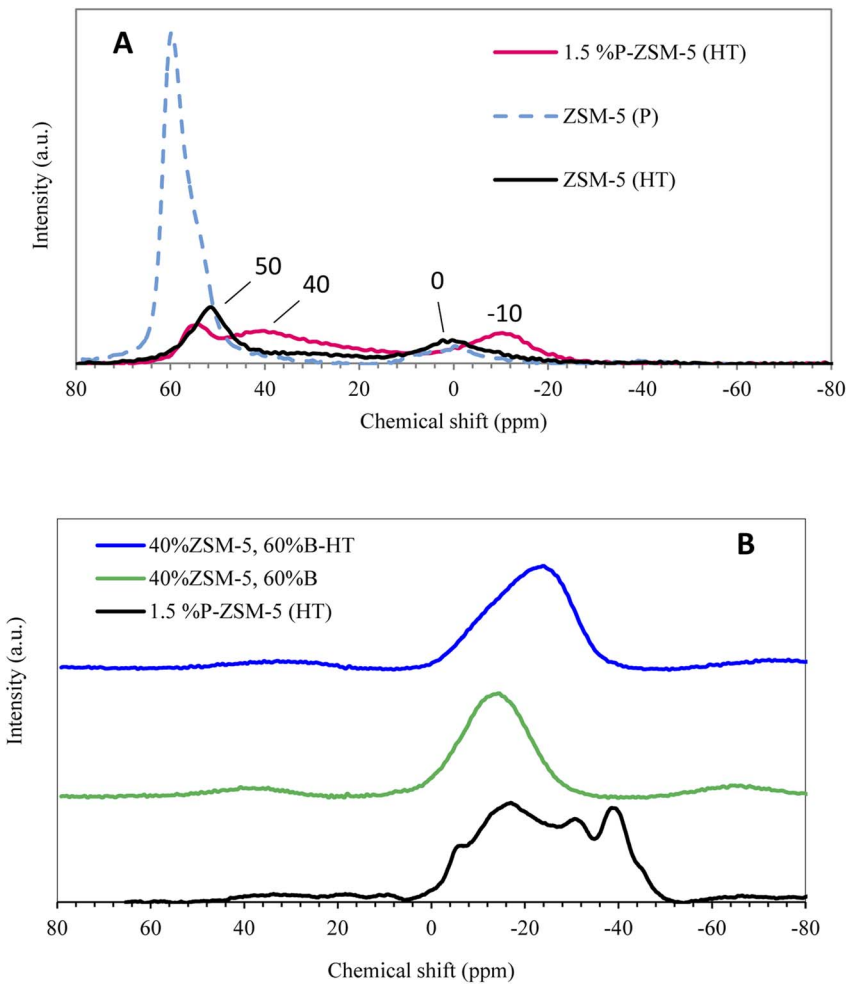

Fig. 3 [A] ^{27}Al MAS NMR spectra of ZSM-5 (P), ZSM-5-HT, and 1.5% P-ZSM-5-HT. [B] ^{31}P MAS NMR spectra of 1.5% P-ZSM-5-HT as reference, 40% ZSM-5-60%B and 40% ZSM-5-60%B-HT.

aluminophosphate molecules, which were retained even after hydrothermal treatment by steam.[59] The interaction of phosphorus with extruded zeolite with binder showed only one wide peak as a result of the high aluminum content of the binder, similar to observations reported earlier by Song *et al.*[36] They suggested that the ^{31}P resonance mainly resulted from the interaction between the binder and phosphorus due to a large amount of aluminum in the binder.[36]

3.5 Reforming reaction of dodecane and heavy naphtha to gasoline

3.5.1 The effect of the zeolite structure on conversion and product selectivity. The catalytic activity of each catalyst was investigated at a temperature of 350 °C using dodecane as the feedstock. The effect of the zeolite structure on dodecane conversion was examined by testing the extruded zeolite of ZSM-5 mixed with binder. Fig. 4A illustrates dodecane conversion over the catalysts with time-of-stream. The medium catalytic pores of 40% ZSM-5 in 60% binder achieved the highest activity with an initial dodecane conversion of 66% and slightly decreased to 54% after 8 h. Fig. 4B shows that the pore selectivity of modified zeolites of 40% ZSM-5 in 60% binder exhibited higher selectivity of paraffin and olefin (~58%), which indicated that the pores of modified zeolites favor monomolecular reaction through β-scission of dodecane.[42,47] While bimolecular pathway was associated with the reaction *via* modified zeolite pore shape selectivity, and it promoted higher iso-paraffin products from isomerization reaction than the cyclization reaction for aromatics and naphthene products.[44–46]

In order to understand the effect of ZSM-5 zeolite pore shape selectivity and reactivity in dodecane conversion, the catalyst of parent ZSM-5 (P) was studied. Fig. 4A shows that ZSM-5 (P) provided higher dodecane conversion (72%) during the first hour of the reaction, then sharply dropped to 32% after 8 h. The best performance in terms of stability and conversion was delivered by the sample impregnated with phosphorus and hydrothermally treated 40% ZSM-5 with 60% binder. Fig. 4B showed the pore selectivity of parent ZSM-5 (P) favored the

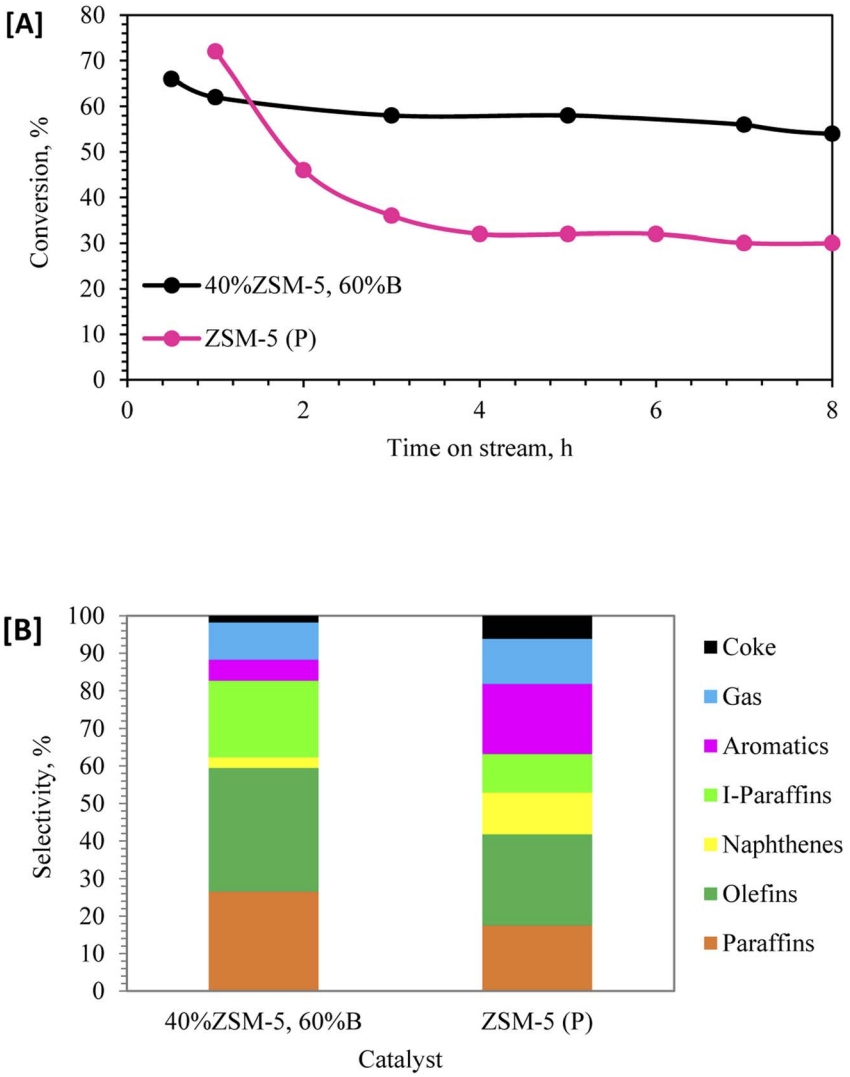

Fig. 4 [A] Dodecane conversion and [B] selectivity at 350 °C: ZSM-5 (P), and 40% ZSM-5 in 60% binder and hydrothermally treated (with steam).

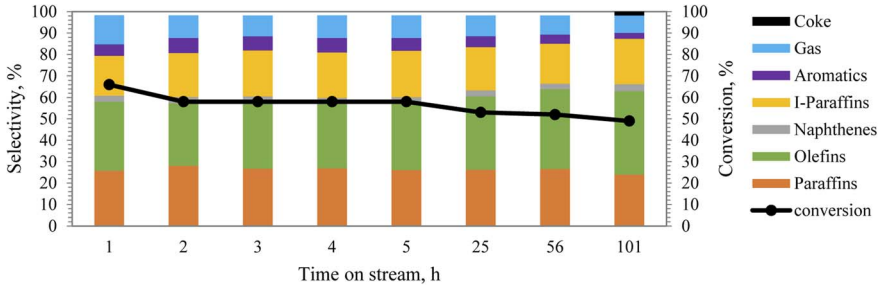

Fig. 5 PIONA analysis and dodecane conversion over the modified catalysts of 40% ZSM-5 in 60% binder.

cyclization reaction to produce aromatic and naphthene products through the bimolecular reaction pathway[43] more than the monomolecular reaction products. The catalysts of 40% ZSM-5 in 60% binder followed different reaction pathways, and the pore selectivity of zeolite favored the monomolecular reaction through β-scission of dodecane[60,61] and promoted the formation of higher paraffin and olefin products.[43,47,61] Fig. 1S (ESI†) shows the schematic diagram of dodecane reforming through the carbonium ions *via* phosphate-modified ZSM-5 zeolite catalyst.

3.5.2 Time-on-stream of dodecane conversion by modified zeolite of ZSM-5 in binder. Time-on-stream dodecane conversion and PIONA analysis were conducted to determine the pore shape selectivity of dodecane of the modified 40% ZSM-5 in 60% binder. The hydrothermally treated phosphorus modified zeolite attained high activity and stability, as demonstrated in Fig. 5, which shows the initial conversion of 66% that decreased to 49% after 101 h. The PIONA analysis demonstrated that the catalyst favored the monomolecular cracking reaction pathway producing high paraffin and olefin selectivity *via* carbonium ions and the β-scission pathway. The modified zeolite showed low selectivity towards bimolecular reactions and produced less than 10% aromatics and naphthenes. On the other hand, the selectivity towards transalkylation and isomerization reactions was higher in the range of 20% and was almost stable during the 101 h run. In addition, the catalyst maintained its stability throughout the run, indicating that the presence of phosphorus oxide was very crucial to resisting coke formation.[34,36] As previously shown, the catalyst acidity was reduced after hydrothermal treatment with steam to a level where the catalyst was still able to crack the dodecane through a monomolecular reaction. Such reduction in catalyst acidity could also be the reason that coke formation was delayed, and the bimolecular reaction was terminated, as aromatics could agglomerate to form coke on the catalyst active sites.[57]

3.6 Heavy naphtha conversion and product distribution

Catalytic reforming of straight run heavy naphtha, obtained from atmospheric distillation, was carried out over the hydrothermally treated (with steam) 40% ZSM-5 in 60% binder catalyst by using similar reaction conditions to dodecane conversion. In addition, the effect of steam on the product distribution was also investigated by co-feeding 10% steam of the total heavy naphtha feed. The straight run heavy naphtha was obtained from atmospheric distillation, having a low research octane number (RON) number of 51 and sulfur content of around 1100 ppm. Heavy naphtha feed consists of 29% paraffin, 1.7% olefins, 27% iso-paraffin, 4.5% naphthene, and 35% aromatics, and 2.8% unidentified peaks.

Results from the PIONA analysis performed on the reformate product from the reforming zeolite activity tests are illustrated in Fig. 6 and 7. It was observed from the results that the catalyst was mainly targeting the paraffinic compounds, as they were reduced initially from 29% to 6.3%, which indicates that the paraffin conversion reached almost 80% during the first hour. After 22 h of operation, the conversion decreased to 37.5%, which was lower than the dodecane conversion at the same time. This could be due to the presence of aromatics in the feedstock, which could potentially agglomerate to block the catalyst pores and deactivate the catalyst gradually. Although the aromatic content in the product increased by around 41%, only a slight increase in the olefin content was observed, as shown by the product distribution in Fig. 6.

On the other hand, the conversion of the paraffin increased to 86.7% in the presence of 10% steam with feedstock (Fig. 7) and then decreased to 69.5% after 22 h of operation. In addition, aromatic content increased by 47% initially, then it decreased to 34.5%, and the coke content was lower than naphtha reforming without steam (Table 3). This suggests that steam helped the zeolite to be more selective towards cyclization and assisted in desorbing the aromatics very quickly out of

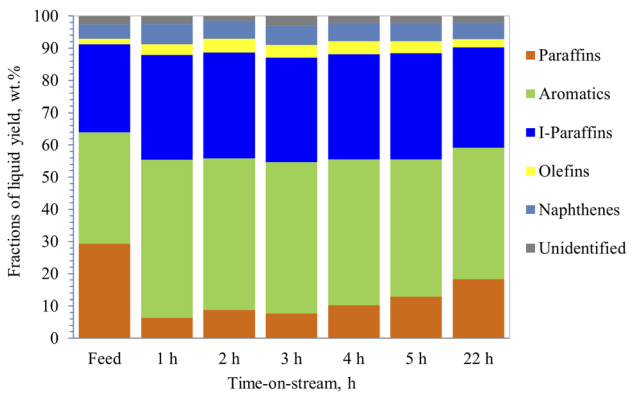

Fig. 6 PIONA analysis of produced hydrocarbons from heavy naphtha over 40% ZSM-5 in 60% binder at 350 °C, without steam, space velocity 4 h^{-1}.

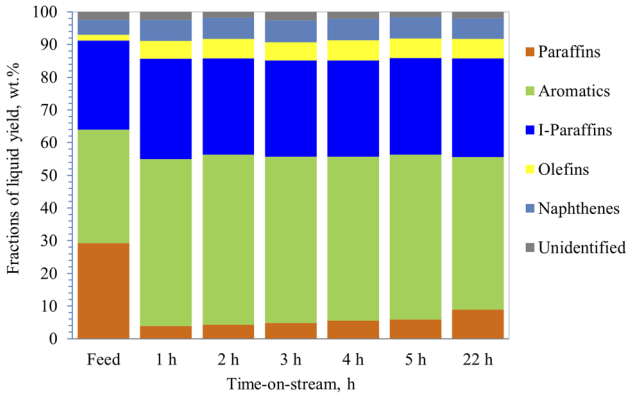

Fig. 7 Additional PIONA production made from heavy naphtha, reaction temp. 350 °C, with 10% steam added to the feed, space velocity 4 h^{-1} *via* 40% ZSM-5 in 60% binder.

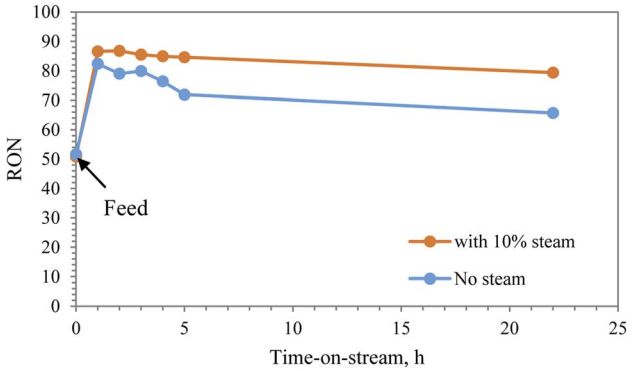

Fig. 8 Increase of RON *vs.* the time-of-stream by using modified 40% ZSM-5 in 60% binder.

Table 3 Material balance of heavy naphtha conversion

Sample ID	Reformate liquid yield (%)	Gas yield (%)	Coke yield (%)
Heavy naphtha reforming without steam	87.6	7.9	4.5
Heavy naphtha reforming in the presence of steam	89.2	7	3.8

the pores, preventing them from blocking the pores, and reducing the coke formation rate, and thus, maintaining the stability of the catalyst. Similar observations were made by Corma *et al.*,[62] where they concluded that steam acts as a diluent that inhibits further coke formation. Furthermore, the rate of bimolecular reactions decreases in the presence of steam and thus contributes to lower formation of coke precursors. Corma *et al.*[62] suggested that the steam helps in reducing the activation energies of the reactions allowing them to proceed faster. Iso-paraffins were the second dominant group in the products from heavy naphtha reforming over the modified 40% ZSM-5 in 60% binder, whereas the naphthene yields were very low. The main products from dodecane catalytic cracking were produced *via* monomolecular cracking resulting in the formation of paraffin and olefins. Unlike dodecane cracking, the main products obtained from heavy naphtha reforming were formed through bimolecular reactions occurring inside the zeolite pores allowing the paraffin and olefins to further react and produce aromatics, iso-paraffins, and naphthenes. Whereas the free radicals from β-scission were affected by the surrounding molecules and did not overcome the cage effect of the feed-stock,[63,64] and cracked molecules went *via* bimolecular reactions through zeolite pores.[64]

Research octane number (RON) is one of the most important parameters to characterize the gasoline reformate. It is used globally to determine the performance of the engine, where gasoline with a high octane number can withstand more compressions prior to ignition. The RON number of straight run heavy naphtha used in the experiments was 51. The RON number was improved significantly after reforming in the presence of steam, reaching 90 after 1 h and then maintained at 80 after 22 h. In the absence of steam, the RON increased to 82 and then dropped to 66 as a result of catalyst deactivation, as shown in Fig. 8.

Eventually, heavy naphtha reforming through zeolite pore shape selectivity followed reaction pathways different from those observed in the dodecane conversion study. The study observed that the addition of 10% steam injected with naphtha feed resulted in a slight increase in aromatic content that remained stable throughout the experiment, with only a slight decline after 22 h, as noticed in Fig. 7. This implies that steam assisted the reactive zeolite pores in performing more cyclization reactions. Specifically, the results suggest that steam helped in suppressing coke formation over the active sites in the acidic pores of the modified ZSM-5 in binder with phosphorus oxide (40% ZSM-5 with 60% binder). The iso-paraffin fraction was shown to be the second dominant product from the reforming of heavy naphtha over the modified 40% ZSM-5 in 60% binder, with low additional yields of naphthenes. The bimolecular reaction of naphtha reforming in the zeolite pores was a dominant reaction pathway than the monomolecular cracking reaction pathway. Thus, olefins and paraffin were produced in lower yields, which was different from observations made in the dodecane conversion study.

The overall conversion of heavy naphtha to produce gasoline reformate was evaluated by the research octane number (RON). The conversion of heavy naphtha over modified zeolite catalyst alongside co-feeding 10% steam led to achieving a higher octane number, which increased from 51 to 86 and then decreased to 80 with time-on-stream, as shown in Fig. 7. Heavy naphtha reforming without steam also resulted in an initial increase in the octane number to 82. However, it drastically decreased to 66 after 20 h. Therefore, steam improved the catalytic stability and reduced coke[62] formation rate resulting in a higher yield of aromatics and consequently higher octane number.

The study highlighted the importance of pore shape selectivity and several modifications, including steaming and phosphorus oxide impregnation. The modified zeolite of ZSM-5 in

the binder showed higher activity and selectivity towards monomolecular products from dodecane. In addition, the modifications improved the conversion stability with a low deactivation rate. Although hydrothermal treatment with steam reduced the acidity of 40% ZSM-5 in 60% binder catalyst, mainly Brønsted acid sites, by 50%, the catalyst showed higher selectivity towards olefin and paraffin products during the conversion of dodecane. This indicated that the catalyst favored monomolecular cracking, where the products accounted for 70% of the dodecane conversion. The tetrahedrally coordinated peak of phosphorus-aluminum species in the framework of ZSM-5 confirmed that phosphorus was successfully loaded to the framework. Such impregnation improved the catalyst stability in dodecane conversion by decreasing the coke formation rate.

However, the heavy naphtha reforming over the modified 40% ZSM-5 in 60% binder by the hydrothermal treatment and phosphorus impregnation showed more selectivity towards the bimolecular reaction, which may be assisted by the increase in the Lewis acid sites after hydrothermal treatment with steam. Furthermore, the products from monomolecular cracking from β-scission were affected by the surrounding molecules and did not overcome the cage effect of feedstock,[63,64] which were elevated to further reactions, including cyclization and isomerization *via* zeolite pores to produce more aromatics and iso-paraffins. The zeolite pore shape selectivity slightly improved and maintained the cyclization reaction when co-feeding 10% steam with heavy naphtha feedstock.

4. Conclusions

This research work investigated the effect of the modification technique on zeolite shape selectivity reaction to enhance aromatic and iso-paraffin production during naphtha reforming. Modified zeolite with phosphorus oxide significantly improved the pore shape selectivity of the catalyst, which plays an important role in facilitating monomolecular and bimolecular reactions in naphtha reforming and dodecane conversion. Although dealumination by the hydrothermal treatment did not impact the zeolite crystalline structure, the textural properties and acidity were affected by the treatment. However, the modification showed that the medium pores of ZSM-5 zeolite were significantly enhanced in terms of shape selectivity after hydrothermal treatment with steam. The study revealed that the zeolite shape selectivity and reaction pathways varied with the feedstock type. Furthermore, the addition of steam improved the reaction selectivity towards more cyclization reactions during naphtha reforming. Also, the addition of steam during the reaction suppressed coke formation. Finally, high conversion and steady selectivity were maintained over the modified shape selective catalyst consisting of 40% ZSM-5 and 60% binder, which resulted in attaining a reformate with high research octane numbers (RON).

Conflicts of interest

The authors declare no competing financial interest.

Acknowledgements

The authors would like to acknowledge Saudi Aramco and acknowledge the efforts of Mohammed A. Sanhoob, Dr Qasim Saleem, and Dr Husin Sitepu in analyzing the samples using FTIR, NMR, and XRD.

References

1 M. A. Ershov, *et al.*, Hybrid low-carbon high-octane oxygenated gasoline based on low-octane hydrocarbon fractions, *Sci. Total Environ.*, 2021, **756**, 142715.
2 T. M. M. Abdellatief, M. A. Ershov, V. M. Kapustin, M. A. Abdelkareem, M. Kamil and A. G. Olabi, Recent trends for introducing promising fuel components to enhance the anti-knock quality of gasoline: A systematic review, *Fuel*, 2021, **291**, 120112.
3 A. Z. Yusuf, Y. M. John, B. O. Aderemi, R. Patel and I. M. Mujtaba, Effect of hydrogen partial pressure on catalytic reforming process of naphtha, *Comput. Chem. Eng.*, 2020, **143**, 107090.
4 M. R. Talaghat and M. S. Karimi, Operation parameters effect on yield and octane number for monometallic, bimetallic and trimetallic catalysts in naphtha reforming process, *Energy Sources, Part A*, 2020, **42**(2), 176–193.
5 L. M. Pastrana-Martínez, S. Morales-Torres and F. J. Maldonado-Hódar, A Comparative Study of Aromatization Catalysts: The Advantage of Hybrid Oxy/Carbides and Platinum-Catalysts Based on Carbon Gels, *C*, 2021, **7**(1), 21.
6 H. Elsayed, M. Menoufy, S. Shaban, H. Ahmed and B. Heakal, Optimization of the reaction parameters of heavy naphtha reforming process using Pt-Re/Al2O3 catalyst system, *Egypt. J. Pet.*, 2017, **26**, 885.
7 E. N. Al-Shafei, *et al.*, Effect of zeolite structure and addition of steam on naphtha catalytic cracking to improve olefin production, *Fuel*, 2022, **321**, 124089, DOI: **10.1016/j.fuel.2022.124089**.
8 S. Bahatia, *Zeolite Catalysis Principles and Application*, ch. 1, 9 & 10, p. 239.
9 E. N. Shafei, A. Masudi, Z. H. Yamani and O. Muraza, Acidity modifications of nanozeolite-Y for enhanced selectivity to olefins from the steam catalytic cracking of dodecane, *RSC Adv.*, 2022, **12**(28), 18274–18281.
10 S. Alipour, Rcecent advances in naphtha catalytic cracking by nano ZSM-5: a review, *Chin. J. Catal.*, 2016, **37**, 671.
11 M. A. Sanhoob, *et al.*, Catalytic Cracking of n-Dodecane to Chemicals: Effect of Variable-Morphological ZSM-5 Zeolites Synthesized Using Various Silica Sources, *ACS Omega*, 2022, **7**(12), 10317–10329.
12 G. A. Nasser, *et al.*, Nano BEA zeolite catalysts for the selective catalytic cracking of n-dodecane to light olefins, *RSC Adv.*, 2021, **11**(14), 7904–7912.
13 P. Kooyman, P. Waal and H. Bekkum, *Zeolites*, 1997, **18**, 50.
14 L. Jin, H. Hu, X. Wang and C. Liu, Methylation of 2-methylnaphthalene with methanol to 2,6-

dimethylnaphthalene over ZSM-5 modified by Zr and Si, *Ind. Eng. Chem. Res.*, 2006, **45**, 3531.
15 S. Han, D. Shihabi and C. Chang, Selective removal of surface acidity in ZSM-5 zeolite using (NH4)2SiF6 treatment, *J. Catal.*, 2000, **196**, 375.
16 P. Zhang, Y. Yang, Z. Li, B. Liu and C. Hu, Preparation, Characterization and Naphtha Aromatization Performance of the Catalytic Reforming Catalyst Pt/MY (M = Mg, Ba or Ce), *Catal. Today*, 2020, **353**, 146–152.
17 N. S. Ahmedzeki, B. A. Al-Tabbakh, M. B. Antwan and S. Yilmaz, Heavy naphtha upgrading by catalytic reforming over novel bi-functional zeolite catalyst, *React. Kinet., Mech. Catal.*, 2018, **125**(2), 1127–1138.
18 S. Karakoulia, E. Heracleous and A. Lappas, Mild hydroisomerization of heavy naphtha on mono-and-bi-metallic Pt and Ni catalyst supported on Beta zeolite, *Catal. Today*, 2020, **355**, 746–756.
19 M. Fedyna, M. Śliwa, K. Jaroszewska and J. Trawczyński, Effect of zeolite amount on the properties of Pt/(AlSBA-15+ Beta zeolite) micro-mesoporous catalysts for the hydroisomerization of n-heptane, *Fuel*, 2020, **280**, 118607.
20 M. H. M. Ahmed, *et al.*, Hydrothermal Stabilization of Rich Al–BEA Zeolite by Post-Synthesis Addition of Zr for Steam Catalytic Cracking of n-Dodecane, *Energy Fuels*, 2018, **32**(4), 5501–5508, DOI: **10.1021/acs.energyfuels.8b00087**.
21 A. Al-Shammari, *et al.*, Catalytic cracking of heavy naphtha-range hydrocarbons over different zeolites structures, *Fuel Process. Technol.*, 2014, **122**, 12–22.
22 Y. Wang, T. Yokoi, S. Namba and T. Tatsumi, Effects of dealumination and desilication of beta zeolite on catalytic performance in *n*-hexane cracking, *Catalysts*, 2016, **6**, 8.
23 V. G.-A. A. Corma and A. Orchillés, The role of pore topology on the behaviour of FCC zeolite additives, *Appl. Catal., A*, 1999, **187**, 245.
24 W. Haag, R. Lago and P. Weisz, The active site of acidic aluminosilicate catalysts, *Nature*, 1984, **309**, 589.
25 A. O. A. Corma, Current views on the mechanism of catalytic cracking, *Microporous Mesoporous Mater.*, 2000, **35**, 21.
26 J. Wan, *et al.*, A ZSM-5 based catalyst for efficient production of light olefins and aromatics from fluidized-bed naphtha catalytic cracking, *Catal. Lett.*, 2008, **124**, 150.
27 M. H. M. Ahmed, O. Muraza, A. K. Jamil, E. N. Shafei, Z. H. Yamani and K.-H. Choi, Steam Catalytic Cracking of n-Dodecane over Ni and Ni/Co Bimetallic Catalyst Supported on Hierarchical BEA Zeolite, *Energy Fuels*, 2017, **31**(5), 5482–5490.
28 M. A. Sanhoob, U. Khalil, E. N. Shafei, K.-H. Choi, T. Yokoi and O. Muraza, Steam cracking of green diesel (C12) to BTX and olefins over silane-treated hierarchical BEA, *Fuel*, 2020, **263**, 116624.
29 A. Talebian-Kiakalaieh and S. Tarighi, Synthesis of hierarchical Y and ZSM-5 zeolites using post-treatment approach to maximize catalytic cracking performance, *J. Ind. Eng. Chem.*, 2020, **88**, 167–177.
30 X. Zhao, X. Guo and X. Wang, Characterization of modified nanoscale ZSM-5 catalyst and its application in FCC gasoline upgrading process, *Energy Fuels*, 2006, **20**, 1388.
31 S. Almutairi, B. Mezari, E. Pidko, P. Magusin and E. Hensen, Influence of steaming on the acidity and the methanol conversion reaction of HZSM-5 zeolite, *J. Catal.*, 2013, **307**, 194.
32 P. Wang, L. Chen, J. Xie, H. Li, C. Au and S. Yin, Enhanced catalytic performance in CH3Br conversion to benzene, toluene, and xylene over steamed HZSM-5 zeolites, *Catal. Sci. Technol.*, 2017, **7**, 2559.
33 X. Meng, Z. Lian, X. Wang, L. Shi and N. Liu, Effect of dealumination of HZSM-5 by acid treatment on catalytic properties in non-hydrocracking of diesel, *Fuel*, 2020, **270**, 117426.
34 H. V. Bij and B. Weckhuysen, Phosphorus promotion and poisoning in zeolite-based materials: synthesis, characterisation and catalysis, *Chem. Soc. Rev.*, 2015, **44**, 7428.
35 M. Cardoso, D. Rosas and L. Lau, Surface P and Al distribution in P-modified ZSM-5 zeolites, *Adsorption*, 2006, **11**, 577.
36 Y. Song, *et al.*, ZSM-5 extrudates modified with phosphorus as a super effective MTP catalyst: Impact of the acidity on the binder, *Fuel Process. Technol.*, 2017, **168**, 105–115.
37 M. A. Sanhoob, O. Muraza, E. N. Shafei, T. Yokoi and K.-H. Choi, Steam catalytic cracking of heavy naphtha (C12) to high octane naphtha over B-MFI zeolite, *Appl. Catal., B*, 2017, **210**, 432.
38 A. Ishihara, K. Inui, T. Hashimoto and H. Nasu, Preparation of hierarchical β and Y zeolite-containing mesoporous silica-alumina and their properties for catalytic cracking of n-dodecane, *J. Catal.*, 2012, **295**, 81.
39 X. B. A. Samanta, B. Robinson, H. Chen and J. Hu, Conversion of light alkanes to value-added chemicals over ZSM-5/metal promoted catalysts, *Ind. Eng. Chem. Res.*, 2017, **56**, 11006.
40 Z. Ismagilov, E. Matus and L. Tsikoza, Direct conversion of methane on Mo/ZSM-5 catalysts to produce benzene and hydrogen: achievements and perspectives, *Energy Environ. Sci.*, 2008, **1**, 526.
41 D. Seddon, Paraffin oligomerisation to aromatics, *Catal. Today*, 1990, **6**, 351.
42 A. A. Al-Absi and S. S. Al-Khattaf, Conversion of Arabian light crude oil to light olefins *via* catalytic and thermal cracking, *Energy Fuels*, 2018, **32**(8), 8705–8714.
43 P. Wang, S. Wang, Y. Yue, T. Wang and X. Bao, Effects of acidity and topology of zeolites on the n-alkane conversion at low reaction temperatures, *Microporous Mesoporous Mater.*, 2020, **292**, 109748.
44 M. Alabdullah, *et al.*, One-step conversion of crude oil to light olefins using a multi-zone reactor, *Nat. Catal.*, 2021, **4**(3), 233–241.
45 M. Alabdullah, *et al.*, Composition-performance Relationships in Catalysts Formulation for the Direct Conversion of Crude Oil to Chemicals, *ChemCatChem*, 2021, **13**(7), 1806–1813.
46 J. Jiang, J. Yu and A. Corma, Extra-large-pore zeolites: bridging the gap between micro and mesoporous structures, *Angew. Chem., Int. Ed.*, 2010, **49**(18), 3120–3145.

47 A. Corma, F. V. Melo, L. Sauvanaud and F. Ortega, Light cracked naphtha processing: Controlling chemistry for maximum propylene production, *Catal. Today*, 2005, **107**, 699–706.

48 A. Al-Ani, C. Freitas and V. Zholobenko, Nanostructured large-pore zeolite: The enhanced accessibility of active sites and its effect on the catalytic performance, *Microporous Mesoporous Mater.*, 2020, **293**, 109805.

49 S. Polovina, M. Vojtech, I. Dejanović, A. Grujić and M. Stijepović, Modeling a reaction section of a commercial continuous catalytic reformer, *Energy Fuels*, 2018, **32**(5), 6378–6396.

50 S. Ebrahimian, D. Iranshahi and A. Bahmanpour, A novel reactor concept for thermal integration of naphtha reforming with propane ammoxidation, *Chem. Eng. Process.*, 2019, **146**, 107659.

51 S. Soltanali, S. R. S. Mohaddecy, M. Mashayekhi and M. Rashidzadeh, Catalytic upgrading of heavy naphtha to gasoline: Simultaneous operation of reforming and desulfurization in the absence of hydrogen, *J. Environ. Chem. Eng.*, 2020, **8**(6), 104548.

52 N. S. Ali and T. H. Aboul-Fotouh, The Effect of Compositions (PIONA) on the Octane Numbers of Environmental Gasolines of Reformate, Isomerate and Hydrocracked Naphtha Blends by Using GC, *Int. J. Oil, Gas Coal Eng.*, 2017, **5**(6), 167–174.

53 J. Balakrishnan and S. Ekambaram, A novel method characterisation of gasoline hydrocarbon on research and motor octane number, *Mater. Today: Proc.*, 2020, **21**, 1026–1030.

54 A. A. Lappas, D. K. Iatridis, M. C. Papapetrou, E. P. Kopalidou and I. A. Vasalos, Feedstock and catalyst effects in fluid catalytic cracking–Comparative yields in bench scale and pilot plant reactors, *Chem. Eng. J.*, 2015, **278**, 140–149.

55 M. A. Sanhoob, O. Muraza, E. N. Shafei, T. Yokoi and K. H. Choi, Steam catalytic cracking of heavy naphtha (C12) to high octane naphtha over B-MFI zeolite, *Appl. Catal., B*, 2017, **210**, 432–443.

56 G. Heitmann, G. Dahlhoff and W. Hölderich, Modified Beta zeolites as catalysts for the Beckmann rearrangement of cyclohexanone oxime, *Appl. Catal., A*, 1999, **185**, 99.

57 Y. Liao, M. d'Halluin, E. Makshina, D. Verboekend and B. F. Sels, Shape selectivity vapor-phase conversion of lignin-derived 4-ethylphenol to phenol and ethylene over acidic aluminosilicates: Impact of acid properties and pore constraint, *Appl. Catal., B*, 2018, **234**, 117–129.

58 P. Wang, *et al.*, Insights into the reaction pathway of n-butane conversion over HZSM-5 zeolite at low temperature, *Appl. Catal., A*, 2019, **584**, 117135.

59 J. Hodala, A. Halgeri and G. Shanbhag, Phosphate modified ZSM-5 for shaped-selective synthesis of *para*-diethylbenzene: Role of crystal size and acidity, *Appl. Catal., A*, 2014, **484**, 8–16.

60 H. Krannila, W. O. Haag and B. C. Gates, Monomolecular and bimolecular mechanisms of paraffin cracking: n-butane cracking catalyzed by HZSM-5, *J. Catal.*, 1992, **135**(1), 115–124.

61 E. N. Al-Shafei, *et al.*, Naphtha catalytic cracking to olefins over zirconia-titania catalyst, *React. Chem. Eng.*, 2022, **7**(1), 123–132.

62 A. Corma, J. Mengual and P. J. Miguel, Steam catalytic cracking of naphtha over ZSM-5 zeolite for production of propene and ethene: Micro and macroscopic implications of the presence of steam, *Appl. Catal., A*, 2012, **417**, 220–235.

63 I. V Khudyakov, P. P. Levin and A. F. Efremkin, Cage Effect under Photolysis in Polymer Matrices, *Coatings*, 2019, **9**(2), 111.

64 Y. Che, M. Yuan, Y. Qiao, Q. Liu, J. Zhang and Y. Tian, Fundamental study of hierarchical millisecond gas-phase catalytic cracking process for enhancing the production of light olefins from vacuum residue, *Fuel*, 2019, **237**, 1–9.